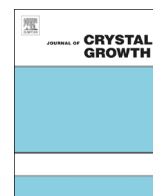




ELSEVIER

Contents lists available at ScienceDirect

Journal of Crystal Growth

journal homepage: [www.elsevier.com/locate/jcrysgr](http://www.elsevier.com/locate/jcrysgr)

# Parabolic tailored-potential quantum-wires grown in inverted pyramids

M. Lazarev<sup>a,\*</sup>, J. Szeszko<sup>a</sup>, A. Rudra<sup>a</sup>, K.F. Karlsson<sup>b</sup>, E. Kapon<sup>a</sup><sup>a</sup> Laboratory of Physics of Nanostructures, Ecole Polytechnique Fédérale de Lausanne (EPFL), Switzerland<sup>b</sup> Department of Physics, Chemistry, and Biology, Linköping University, Linköping S-58183, Sweden

## ARTICLE INFO

Available online 13 November 2014

## Keywords:

A3. MOVPE

A2. Patterned growth

A3. Heterostructures

A1. Low dimensional semiconductors

A2. Quantum wires

A1. Photoluminescence

## ABSTRACT

Quasi-one-dimensional AlGaAs quantum wires (QWRs) with parabolic heterostructure profiles along their axis were fabricated using metallorganic vapor phase epitaxy (MOVPE) on patterned (111)B GaAs substrates. Tailoring of the confined electronic states via modification in the parabolic potential profile is demonstrated using model calculations and photoluminescence spectroscopy. These novel nanostructures are useful for studying the optical properties of systems with dimensionality between zero and one.

© 2014 Elsevier B.V. All rights reserved.

## 1. Introduction

Semiconductor quantum wires (QWRs) with tailored heterostructure potential along their axis represent an interesting low-dimensional system, intermediate between one-dimensional (1D) QWRs and 0D quantum dots (QDs). One interest in such systems stems from the possibility it offers for tailoring the degree of quantum confinement of valence band states, which can be used to adjust the admixture between heavy- and light-hole states and the related optical polarization properties [1]. More generally, it makes possible the realization of a variety of quasi-1D potential charge carrier traps with unique features of carrier interactions and single-photon emission [2]. Such quasi-1D systems can be realized based on nano-wires [3], stacked self-assembled QDs [4], or vertical QWRs self-formed in inverted pyramids [5]. The flexibility of the latter approach, implemented using metallorganic vapor phase epitaxy (MOVPE) of GaAs/AlGaAs heterostructures in inverted tetrahedral pyramids etched on (111)B GaAs substrates, has been illustrated in studies of AlGaAs quasi-1D QWRs of different potential shapes [6,7]. Here, we report [8] the realization and the optical properties of such pyramidal AlGaAs QWRs exhibiting parabolic potential profiles extending along their axis. Quantum wires with such parabolic potential variations along their axis would serve as interesting model systems for adjusting the balance between 3D quantum confinement effects and Coulomb interaction, which is important, e.g., for the observation of Wigner correlations in 1D traps of charge carriers [8].

## 2. Fabrication of parabolic quantum wires

The pyramidal QWR structures were grown using MOVPE on (111)B GaAs substrates patterned with inverted tetrahedral pyramids exposing {111}A facets [9]. The substrates were patterned using photolithography and wet etching in 1:100 Br:Methanol solution through a SiO<sub>2</sub> mask. Subsequent growth of AlGaAs heterostructures yields a set of low-dimensional AlGaAs nanostructures inside the pyramids due to characteristic growth rate anisotropy and capillarity-induced Ga–Al segregation [10] (see Fig. 1). Top scanning electron microscopy (SEM) images of the substrates before and after growth are shown in Fig. 2. In particular, a vertical, Ga-rich AlGaAs QWR (VQWR) is formed at the center of the pyramid, laterally bounded by 3 vertical quantum wells (VQWs) that grow on the pyramid wedges and 3 vicinal vertical quantum wells (vicinal VQWs) that are formed between the vicinal-{111}A facets developed during the growth from the initial pyramid sidewalls (see Fig. 2). The lateral dimensions (diameter) of the VQWR are set by the Al–Ga segregation, and are typically 10–20 nm for the structures discussed here [11]. The core of this VQWR has Al content much lower than that in its surroundings, which provides the main change in heterostructure potential for setting the lateral quantum confinement [11]. Similar, but reduced Al–Ga segregation takes place at the wedges of the pyramid, forming the VQW barriers of this VQWR, while even weaker segregation leads to formation of the vicinal-VQW barriers between the vicinal facets. Changing the Al content during growth allows to tailor the bandgap, and with it the confining potential of the QWR, along its axis with monolayer precision. Different QWR potential profiles have already been demonstrated and investigated with this approach, including a dot-in-wire [12], linearly-graded [7] and double-linearly-graded [2] QWR structures. In the current work,

\* Corresponding author. Tel.: +41 78 645 86 26.

E-mail address: [mikhail.lazarev@epfl.ch](mailto:mikhail.lazarev@epfl.ch) (M. Lazarev).

we shaped the nominal Al content  $x$  of the  $\text{Al}_x\text{Ga}_{1-x}\text{As}$  heterostructure to have a parabolic bandgap profile with different gradients, in order to achieve prescribed quasi-1D electron and hole states. This

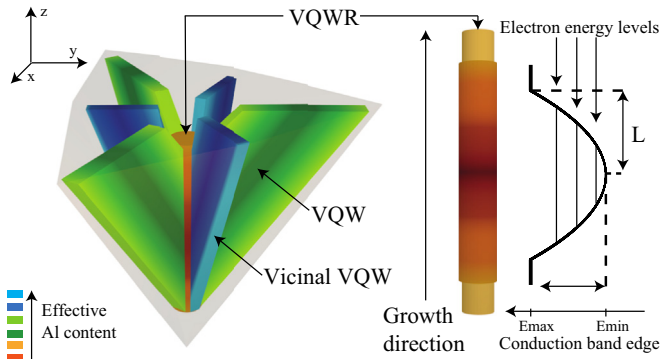


**Fig. 1.** Schematics of the pyramidal nanostructure system formed inside the inverted pyramid (left), and a simplified magnified view of the parabolic quantum wire and its conduction band profile.

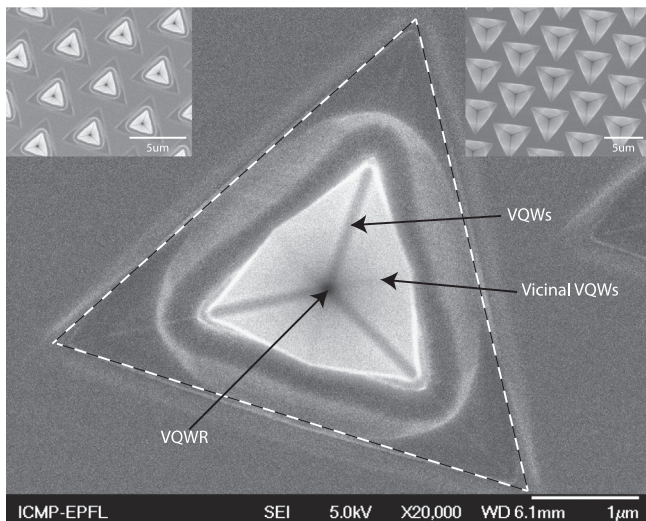


**Fig. 2.** Top SEM image of a pyramidal structure after growth and surface etching  $2L=220$  nm. Left inset shows an array of etched pyramids after growth; the right one shows a patterned substrate before growth.

parabolic section, with nominal Al contents changing between 0.2 and 0.4, was sandwiched between barriers of nominally  $x=0.4$  Al content, thick enough to simulate “infinitely” long QWR barriers. The three parabolic-QWR structures, denoted A, B and C, had a nominal half-length  $L_{\text{nom}}$  of 27.5, 55 and 110 nm, respectively.

The MOVPE growth was carried out at 20 mb in an Aix200 commercial reactor using Trimethylgallium (TMGa) and Trimethylaluminum (TMAI) from Albermarle Cambridge Chemical Co. and Arsine 6N5 Ultima II from Matheson with  $\text{N}_2$  as a carrier gas. The “nominal”  $\text{Al}_x\text{Ga}_{1-x}\text{As}$  growth rates and alloy compositions were calibrated by growing InAs/GaAs superlattice structures and AlGaAs/GaAs heterostructures on planar (100) GaAs substrates. The X ray diffraction (XRD) rocking curves measured for the planar growth were fitted against theoretical curves derived using a dynamical XRD theory. Nominal growth rates close to 0.06 nm/s could be reproducibly obtained using a total reactor flow of 2.36 l/min. The carrier gas injection was adjusted to limit growth rate variations below  $\pm 10\%$  over 2 in. substrates. Inside the pyramids on the patterned substrates, the actual growth rates are enhanced both due to migration of metallorganic species into the pyramids from the (111)B planar parts where they poorly decompose, and the faster growth rate on the {111}A sidewalls as compared to the (100) planes. The vertical growth rate in the pyramids is thus enhanced by a factor  $K$  as compared to the “nominal” growth rate measured on the planar (100) substrates. Comparing cross sectional SEM images of the grown structures, we determined  $K$  to be in the range of 1.8–2.2; a value of  $K=2$  ( $L=2L_{\text{nom}}$ ) was used in the modeling of the electronic states presented below.

Three samples with parabolic QWR structures of different lengths were prepared. Each grown GaAs/AlGaAs heterostructure consisted of a 10 nm thick GaAs buffer layer, a 45 nm  $\text{Al}_{0.75}\text{Ga}_{0.25}\text{As}$  etch-stop layer, a 100 nm  $\text{Al}_{0.4}\text{Ga}_{0.6}\text{As}$  cladding layer followed by an  $\text{Al}_x\text{Ga}_{1-x}\text{As}$  layer where the nominal Al content first decreases from  $x=0.4$  to  $x=0.2$ , then increases back to  $x=0.4$  following a parabolic profile. This profile was obtained by dividing the growth sequence into  $2 \times 20$  steps of equal  $\Delta x$  and linearly grading the Al content  $x$  in each of the segments by adjusting the TMGa and TMAI partial pressures. The growth was then completed by a 45 nm  $\text{Al}_{0.4}\text{Ga}_{0.6}\text{As}$  layer and a 5 nm thick GaAs cap layer. Prior to epitaxial growth, the samples were stabilized at 770 °C (thermocouple reading) under Arsine. The growth temperature was then reduced and the parabolic graded  $\text{Al}_x\text{Ga}_{1-x}\text{As}$  layer was grown at 705 °C under a  $V/III$  ratio close to 1200. Samples A, B and C had the same barriers structure and their parabolic core had actual lengths of  $2L=110$ , 220 and 440 nm, respectively.

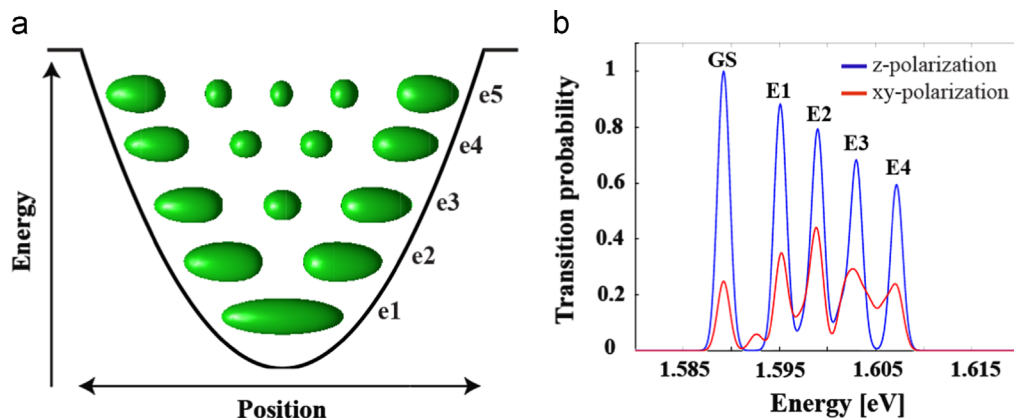


**Fig. 3.** Model calculations for parabolic-QWR B ( $2L=220$  nm). a) Schematic illustration of the conduction band profile along the QWR and electron wavefunction isosurfaces (probability density value 0.00006) of the 5 lowest energy electron states GS–E1–E4. b) Calculated spectra showing strengths of interband transitions between conduction and valence band states. Z-polarization indicates linear polarization along the QWR growth direction, while x–y polarization denotes linear polarization in the plane perpendicular to the QWR growth direction.

### 3. Model of confined states

The electronic conduction band and valence band states were calculated using a model that accounts for the three-dimensional pyramid geometry, including the actual AlGaAs compositions derived from previous characterization work [11]. Using the envelope function approximation, the conduction band was described as a single band, whereas the valence band was modeled based on a  $4 \times 4$  Luttinger Hamiltonian, taking into account valence bands mixing. Coulomb interaction between holes and electrons was included as a perturbation. Some results of the model calculations are illustrated in Fig. 3 for structure B ( $2L=220$  nm). The electron

wavefunctions exhibit harmonic oscillator-like features, with even energy spacing of 3 meV (see Fig. 3(a)). In the valence band, the hole states are characterized by a mixed heavy-hole and light-hole character due to the 3D quantum confinement [13]. The calculated probabilities for transitions between the confined conduction band and valence band states show several main peaks, separated by  $\sim 6$  meV, marked as GS, E1, E2, ...E4 in Fig. 3(b). Modeling of structures A and C yields similar transitions polarized mainly along the QWR growth direction with GS–E1 energy spacing of 11 meV and 3 meV, respectively.

### 4. Photoluminescence spectroscopy

The photoluminescence (PL) spectra of the parabolic VQWR structures were acquired with a micro-PL set up, using photo-excitation with a laser (532 nm wavelength) of a spot size of 1–2  $\mu\text{m}$ . Prior to the PL measurements, the GaAs substrate was removed to increase the excitation and detection efficiency through the a substrate removal process: it consists of flipping the sample and gluing it onto a new substrate using wax before thinning it first by mechanical polishing and then by wet chemical etching in a  $\text{NH}_4\text{OH}:\text{H}_2\text{O}_2$  (1:30) solution to remove the rest of the initial substrate. Single pyramids were excited and the PL was collected in top-view geometry, where the excitation beam and the collection axis are both along the growth direction. Fig. 4 shows the micro-PL spectra measured in this configuration at  $T=10$  K and at moderate excitation levels  $P_{\text{exc}}$  for all three samples. The different spectral features due to emission from the VQWR and the surrounding barriers are indicated, based on previous experiments on similar structures [11]. In Fig. 4 there are 3 types of emission peaks, which we associate with 3 sub-structures in our pyramid, VQWR, VQWs and Vicinal VQWs. Based on cathodoluminescence experiments [11] of previously studied structures, we can identify the main emission peaks in the PL spectra. The first peak at 1.55 eV is associated with the emission from the VQWR, which is in good agreement with our calculations and with the Al content of VQWR according to our segregation model. The other two peaks at 1.654 eV and 1.755 eV originate from the VQWs and the vicinal VQWs respectively. In Fig. 4c, the emission line at 1.61 eV between the VQWR and the VQW emissions, is due – according to our segregation model – to the barrier of the VQWR (of 40% nominal Al content). Magnified views of the emission spectra of the parabolic QWRs are shown in the insets. The features in these spectra correspond to transitions between conduction and valence band states confined by the parabolic potential wells. As expected, the energy separation between these transitions increases with increasing gradient of the parabolic profiles.

The power dependence of the PL spectra of sample B is presented in Fig. 5, focusing on the emission from the parabolic QWR. With increasing excitation level, an increasing number of transitions are visible as a result of state filling. The nearly equal energy spacing of the transitions, 7 meV, corresponds well to the calculated value of  $\sim 6$  meV.

### 5. Conclusions

We employed MOVPE on patterned (111)B GaAs substrates in order to realize AlGaAs QWR structures with tailored potential variations along their axis. In particular, we demonstrated the fabrication of QWRs with parabolic potential profiles of prescribed gradients. Evidence for the formation of harmonic-oscillator like electronic states in these QWRs is provided by micro-PL spectroscopy supported by modeling of the confined states. The realized

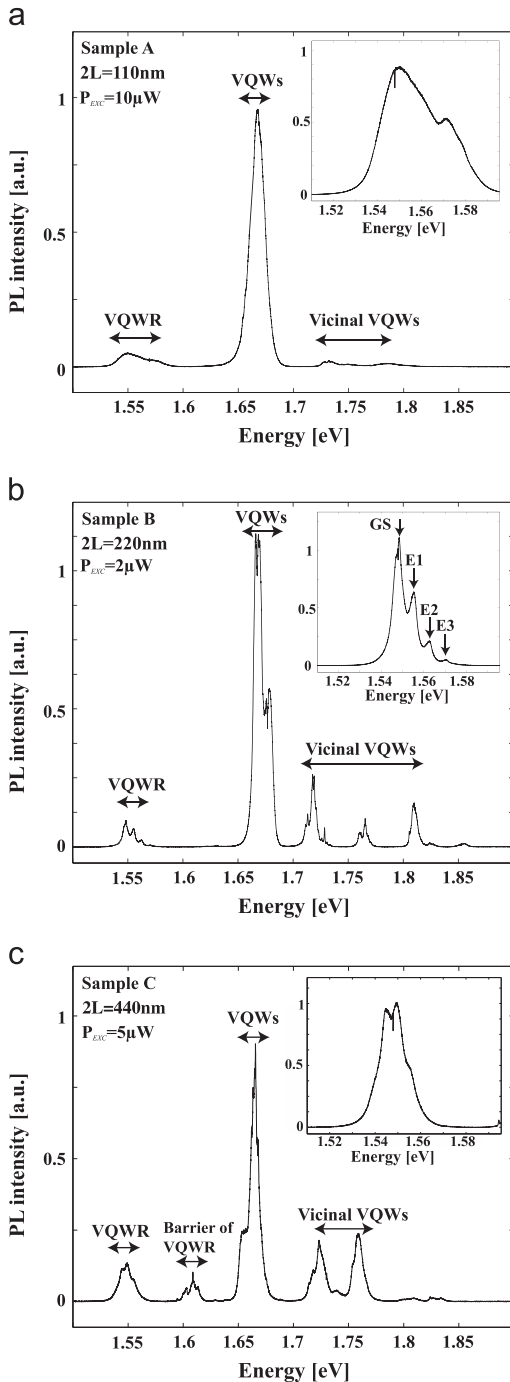
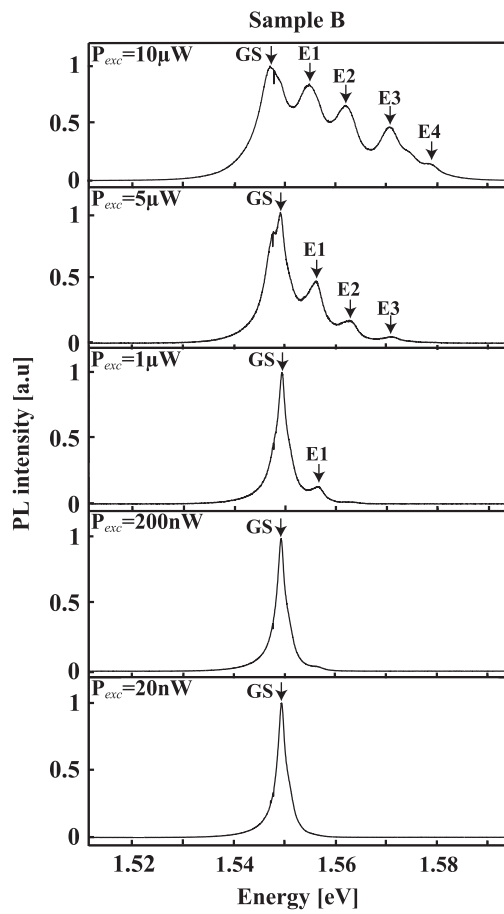


Fig. 4. PL spectra of structures A, B and C measured at the indicated excitation powers  $P_{\text{exc}}$  and at  $T=10$  K. Insets show magnified views of the VQWR emission spectra.



**Fig. 5.** Excitation power dependence of VQWR emission of Structure B ( $2L=220$  nm), measured at  $T=10$  K for different excitation powers.

low-dimensional structures are intermediate between 1D and 0D systems, opening up the possibility for investigating the physics of a novel type of quantum-confined structures.

### Acknowledgment

This work was supported by the Swiss National Science Foundation (Project 200020\_156748 “Semiconductor Quantum Nanophotonics based on Ordered Systems of Quantum Wires and Dots”).

### References

- [1] V. Troncale, K.F. Karlsson, E. Pelucchi, A. Rudra, E. Kapon, *Appl. Phys. Lett.* 91 (2007) 241909.
- [2] J. Szeszko, V.V. Belykh, P. Gallo, A. Rudra, K.F. Karlsson, N.N. Sibeldin, E. Kapon, *Appl. Phys. Lett.* 100 (2012) 211907.
- [3] M.S. Gudiksen, L.J. Lauhon, J. Wang, D.C. Smith, C.M. Lieber, *Nature* 415 (2002) 617.
- [4] J. He, H.J. Krenner, C. Pryor, J.P. Zhang, Y. Wu, D.G. Allen, C.M. Morris, M.S. Sherwin, P.M. Petroff, *Nano Lett.* 7 (2007) 802.
- [5] Q. Zhu, E. Pelucchi, S. Dalessi, K. Leifer, M.-A. Dupertuis, E. Kapon, *Nano Lett.* 6 (2006) 1036.
- [6] Q. Zhu, K.F. Karlsson, M. Byszewski, A. Rudra, E. Pelucchi, Z. He, E. Kapon, *Small* 5 (2009) 329.
- [7] J. Szeszko, V.V. Belykh, A. Rudra, N.N. Sibeldin, E. Kapon, *Appl. Phys. Lett.* 104 (2014) 261905.
- [8] S. Pecker, et al., *Nat. Phys.* 9 (2013) 576.
- [9] A. Hartmann, L. Loubies, F. Reinhardt, E. Kapon, *Appl. Phys. Lett.* 71 (1997) 1314.
- [10] G. Biasiol, E. Kapon, *Phys. Rev. Lett.* 81 (1998) 2962.
- [11] Q. Zhu, J.D. Ganiere, Z.B. He, K.F. Karlsson, M. Byszewski, E. Pelucchi, A. Rudra, E. Kapon, *Phys. Rev. B* 82 (2010) 165315.
- [12] J. Szeszko, Q. Zhu, P. Gallo, A. Rudra, E. Kapon, *Appl. Phys. Lett.* 99 (2011) 091910.
- [13] K.F. Karlsson, V. Troncale, D.Y. Oberli, A. Malko, E. Pelucchi, A. Rudra, E. Kapon, *Appl. Phys. Lett.* 89 (2006) 251113.